

Improving Performance of Dye Sensitized Solar Cells Based On Composite Quasi Solid-State Electrolytes of Poly (ionic liquid) / Ionic liquid / TiO₂.

A. Benabdellah^{1*}, K. Negadi², Y.Chaker², B. Fetouhi², M.Debdab², H.Belarbi², M. Hatti³

^{1,2}Synthesis and Catalysis Laboratory, University of Tiaret, Algeria.

²Department of Electrical Engineering, Laboratory of L2GEGI, University of Tiaret, Algeria.

³ UDES, Solar Equipments Development Unit, Bou Ismail, Tipaza, Algeria.

Corresponding Author Email: abdelkader.benabdellah@univ-tiaret.dz

<https://doi.org/10.14447/jnmes.v24i4.a06>

ABSTRACT

Received: June 21-2021

Accepted: November 30-2021

Keywords:

poly (IL); Ionic liquid; DSSCs; conversion efficiency, long-term stability.

Composite gel electrolytes of poly(IL) /IL/TiO₂ containing poly [1-(hydroxyethyl)-3-vinylimidazolium hydrogen sulfate] (poly [EtOHVIM⁺][HSO₄⁻]) as Poly(IL), 1-butyl-3-methyl- imidazolium hexafluorophosphate ([BMIM] PF₆) as IL and Titanium Dioxide (TiO₂) are prepared for dye-sensitized solar cells (DSSCs), without any volatile organic solvent. The performance of most (DSSCs) based on TiO₂ was limited by the low electron mobility within TiO₂. To produce a much higher power conversion efficiency performance and better long-term stability of the composite electrolyte without TiO₂, a proper amount of TiO₂ was added. Overall power conversion efficiency of 7.46% under simulated AM 1.5 solar spectrum irradiation for (DSSCs) based on the composite electrolytes were showed. This type of composite electrolytes had long-term stability of the (DSSCs), could overcome the drawbacks of volatile liquid electrolytes, and offer a feasible method to fabricate (DSSCs) in future practical applications.

1. INTRODUCTION

Development of efficient dye-sensitized solar cells (DSSCs) by simple methodologies offer immense scope and potential in the global strive towards harvesting solar energy [1, 4].

The uses of liquid electrolytes in fabrication for (DSSCs) by traditional process lead to long-term stability problems because of the leakage and volatility [5]. To solve these problems, some solid electrolytes, such as inorganic p-type semiconductors [6, 7] and organic hole-transport materials [8, 12], have been applied in (DSSCs). Solid-state electrolytes could be reduce the leakage problems, enhance the lifetime and sealing cost of (DSSCs) due to it's a low evaporation rate [13, 15]. It is reported that addition of inorganic nanoparticles into the electrolytes is an effective way to improve the (DSSCs) performance [16, 17]. TiO₂ is the most broadly studied (DSSCs) photoanode material where a highest solar conversion efficiency of 11.2% is reported [18]. The poor penetration into mesoporous TiO₂ is a major problem influenced on the efficiency of solid state electrolytes, due to lower ionic conductivity, poor electron transfer from dye molecules and recombination faster [19, 21]. Therefore, for combining the best of both sides, the development of quasi-solid-state electrolytes, especially gel polymer electrolytes could resolve the problem of the leakage of liquid electrolyte to some extent, because of their complex preparation process, poor mechanical strength, and low thermal stability, but having limitation area when it comes to using them on a commercial scale [22-25].

Ionic liquid (IL) electrolytes are widely used in dye-sensitized solar cells (DSSCs) in place of organic electrolytes for its unique properties such nonvolatile, negligible vapor pressure, excellent thermal stability, broad electrochemical potential window and high ionic conductivity [25, 27]. Nonetheless, (DSSCs) based on (ILs) are prone to leakage, and in order to overcome this problem, polymer gel electrolytes have been developed for (DSSCs) [28–30]. Although polymer gel electrolyte-based (DSSCs) do not suffer from electrolyte loss, they tend to have low power conversion efficiencies attributed to the lower ionic mobility of ions [31, 32].

Poly (ionic liquid) (poly (IL)) as a new class of polymers which combine both the properties of ionic liquid and polymers have attracted much attention in recent years [33-35]. Their using for quasi-solid-state (DSSCs) showed high power conversion efficiency and excellent long term stability [36, 37].

In this work, we present an entirely approach to the fabrication of high performance (DSSCs) by using a composite gel electrolyte containing poly (IL) / IL / TiO₂ as sensitizer and IZO coated FTO glass substrate as a counter electrode are expected to offer good alternative to the expensive dyes along with improvement in environmental and commercial benefits. The (DSSCs) properties were systematically investigated by the influence of TiO₂ content with various amounts. The TiO₂ could be well dispersed in poly (IL) / IL to form quasi-solid-state gel electrolytes, without using any volatile organic solvents. Better performance and stability were obtained for the quasi solid-state (DSSCs) with TiO₂ compared that without TiO₂, which

indicating the poly (IL) / IL / TiO₂ composite gel electrolytes are a promising candidate for (DSSCs) with good durability.

Characterization of electrolytes

The performance of a (DSSCs) is usually influenced by the conductivity of electrolyte, for this, the (DSSCs) based on semi-solid IL electrolytes containing various contents (0 wt%, 1 wt%, 2 wt%, 4 wt%, 6 wt%, 8 wt%) of TiO₂ were prepared respectively. The conductivities of electrolytes containing different content of TiO₂ were measured with a CHI660c electrochemical workstation at room temperature, and the results listed in Table 1.

It can be clearly seen that the incorporation of proper amount of TiO₂ in the composite electrolytes increases the conductivities. For example, the minimal value of the conductivity of electrolyte it reaches $2.84 \times 10^{-3} \text{ S.cm}^{-1}$ by 0 wt% of TiO₂ and increase to the maximum value of $6.72 \times 10^{-3} \text{ S.cm}^{-1}$ by 4 wt% of TiO₂. This explained by formation of ion transportation network in the quasi solid-state electrolyte was favors by the addition of TiO₂, which improved the movement of free ions in a regular direction [38, 39]. However, the conductivity of the quasi solid-state electrolyte was decrease by the excess of TiO₂, indicating potential saturation of ion transport channels formed by the incorporation of TiO₂, and the further their addition could block the formed ion transport channels [39]. Therefore, it is not surprising that excess TiO₂ resulted in low ionic conductivity.

2. EXPERIMENTAL PROCEDURES

2.1. Reagents and instruments

Zinc acetate dihydrate (Zn (CH₃COO)₂ · 2H₂O), indium nitrate trihydrate (In (NO₃)₃ · 3H₂O), absolute Ethanol (C₂H₅OH), and Monoethanolamine (NH₂CH₂CH₂OH) pure products of Sigma-Aldrich were used to prepare In-doped ZnO thin films (IZO). TiO₂ nanoparticles (Titanium (IV) oxide, T-20 nm), acetic acid silver (C₃H₃AgO₃) and iodine were obtained from Sigma-Aldrich. N719 dye, Surlyn (ionomer films of 25- μm thick) and FTO conducting glass (resistance of 20 Ω /square, transmittance of 85 %) were purchased from Dalian Rainbow Solar Technology Development Co.Ltd., Dalian, China. All reagents were of analytical grade and were used as received unless otherwise stated. XRD analysis was carried out using a RAD-3X (Rigaku Corporation, Tokyo, Japan) diffractometer with Cu-K α radiation. The conductivity of the electrolytes was characterized in an ordinary cell composed of Teflon tube and two identical stainless steel electrodes (diameter of 1cm) on a CHI660c electrochemical workstation at room temperature, using the AC impedance method over the frequency range 0.1Hz- 1MHz. The current-voltage (J-V) characteristics were examined by a Keithley model 2400 source meter (Keithley Instruments, Inc. Cleveland, USA) under AM 1.5 solar spectrum irradiation of 100mW/cm².

2.2. Preparation of IZO thin films coated FTO Glass substrate

IZO thin films were prepared by the sol-gel dip-coating method using zinc acetate dihydrate and Indium nitrate trihydrate as starting materials followed the literature [28]. For depositing IZO thin films of high physical properties of

ZnO, 15% of indium was added to solution. The FTO coated glass substrates were cleaned in an ultrasonic bath in acetone, ethanol and distilled water successively. The IZO layers were deposited by immersing a substrate in the solution for 2 min (Dip-coater KSVDCX2), and then dried at high temperature 300 °C for 4 min in an electric furnace (Nabertherm B-180). The procedure from immersing to drying was repeated 15 times, the IZO films were then annealed at 500 °C for 2h to ensure good electrical contact between the IZO films and the FTO coated glass substrates.

2.3. Synthesis of the poly (IL) and IL

Synthesis and characterization of (poly [EtOHVIM⁺] [HSO₄⁻]) as Poly (IL) and [BMIM] PF₆ as IL followed the literature [29, 30].

2.4. Preparation of poly (IL)/IL/TiO₂ composite electrolytes

The liquidelectrolyte was composed of 1M [BMIM] PF₆ (0.1M HF, 0.5 M PF₅, 0.4M PCl₅), 20 wt% of the poly (IL) (based on the weight of the liquid electrolyte) and different amount (0%, 1%, 2%, 4%, 6%, 8%) of TiO₂ was added into the liquid electrolyte and stirred at 60 °C for 4 h, then the homogeneous poly(IL)/IL/ TiO₂ electrolytes were obtained.

2.5. Fabrication of DSSCs

The (DSSCs) were fabricated by using a conventional process according: Dye adsorption was carried out by immersing the IZO working electrodes in N719 dye solution (0.5 mM in ethanol) at room temperature for 24 h, then the IZO electrodes were rinsed with ethanol and dried under nitrogen flow. The Ag counter electrode was prepared by dripping a drop 5 mM of acetic acid silver ethanol solution placed onto FTO glass substrate, followed by annealed at 500°C for 15min. (DSSCs) were fabricated by sandwiching poly(IL)/IL/TiO₂ electrolytes between dye sensitized IZO working electrode and Ag counter electrode, which were using a sheet of a thermoplastic frame (20- μm thick, Surlyn) as a spacer between the two electrodes. The typical active area of the cells was 0.5 cm².

3. RESULTS AND DISCUSSION

3.1 XRD of IZO coated FTO glass substrate

Figure 1 shows the X-ray diffraction pattern for the amorphous IZO semiconductors and at layer deposited on FTO glass substrate. The X-ray diffraction investigations showed that the FTO glass was highly textured, with its (200) axis being perpendicular to the substrate, as one can see in Figure 1.

To better distinguish the patterns acquired from the grown IZO particles, offset (incidence angle close, but slightly different from theta) and grazing incidence (incidence angle = 5°) geometries were used, and the acquired patterns. The XRD pattern of the IZO sample showed a smooth surface composed of small grains (Figure 1). For this film, the (110) peak at 33.54° is dominant. This preferential (110) orientation is unique among the reported high-quality coated IZO films, of which the majority exhibited a (101) texture

[31, 32]. It should be noted that, apart from the solution composition and deposition conditions, the use of a seeding layer can also influence the texture of the film [33].

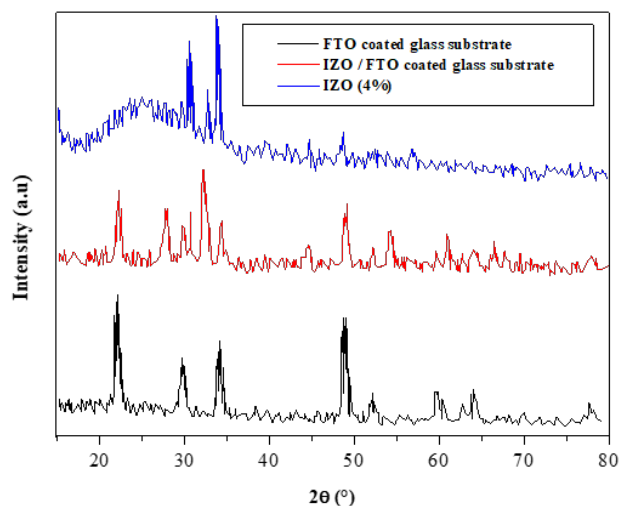


Figure 1. XRD spectra of IZO and IZO coated FTO glass substrate

3.2. Morphological properties of IZO coated FTO glass substrate

Properly cross-sections images of the two films (FTO coated glass substrate and IZO coated FTO glass substrate) were performed with a Tescan Lyra3 FEG-SEM combining high resolution and high-performance Ga focused ion beam (FIB) required for optical applications (Figure 2).

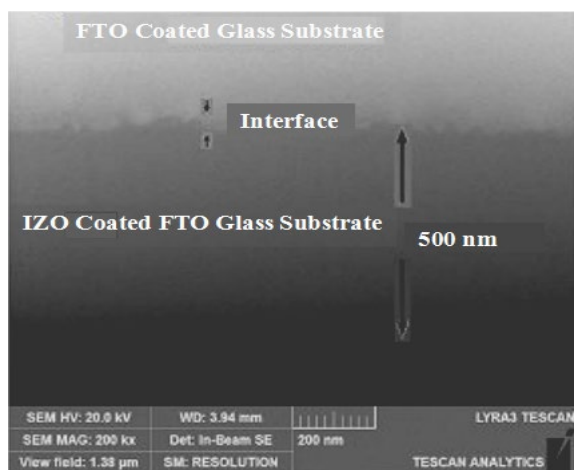


Figure 2. Cross-sections images of FTO coated glass substrate and IZO coated FTO glass performed by FEG-SEM

The thickness observed by FEG-SEM of the two films is homogenous and surfaces are very smooth. In the two samples, similar rough interfaces between the IZO thin film and the FTO coated glass substrate are observed. However the IZO thin film appears to be denser than that of FTO coated glass substrate. The deposited films present more porosity near the surface. The texture of the film cross-section is finer for IZO.

3.3. Characterization of electrolytes

The DSSCs based on semi-solid IL electrolytes containing various contents (0 wt%, 1 wt%, 2 wt%, 4 wt%, 6 wt%, 8 wt%) of TiO₂ were prepared respectively. All the electrolytes are quasi-solid-state gels at room temperature. The performance of a DSSC is usually influenced by the conductivity of electrolyte. The conductivities of electrolytes containing different content of TiO₂ were measured with a CHI 660c electrochemical workstation at room temperature, and the results listed in Table 1.

Table 1. Photovoltaic performance parameters of the DSSCs based on electrolytes content (0 wt%, 1 wt%, 2 wt%, 4 wt%, 6 wt%, 8 wt%) of TiO₂ measured under AM 1.5 solar spectrum irradiation of 100 mW cm⁻²

Cells content	Conductivity	J _{sc}	V _{oc}	FF	η
TiO ₂ (wt%)	(10 ⁻³ S. cm ⁻¹)	(mA. cm ⁻²)	(mV)		(%)
0 wt%	2.84	7.32	0.96	0.72	1.24
1 wt%	3.46	8.86	1.03	0.81	2.48
2 wt%	4.21	15.96	1.13	0.85	5.51
4 wt%	6.72	18.84	1.16	0.89	7.46
6 wt%	6.16	11.92	1.11	0.83	4.42
8 wt%	5.12	7.86	0.99	0.76	3.12

It can be clearly seen that the incorporation of proper amount of TiO₂ in the composite electrolytes increases the conductivities. For example, the minimal value of the conductivity of electrolyte it reaches 2.84 × 10⁻³ S.cm⁻¹ by 0 wt% of TiO₂ and increase to the maximum value of 6.72 × 10⁻³ S.cm⁻¹ by 4 wt% of TiO₂. The formation of ion transportation network in the quasi solid-state electrolyte was favored by the addition of TiO₂ [34, 35]. However, the conductivity of the quasi solid-state electrolyte was decreased by the excess of TiO₂, indicating potential saturation of ion transport channels formed by the incorporation of TiO₂, and the further their addition could block the formed ion transport channels [35].

3.4. Characterization of DSSCs

Photocurrent density-voltage characteristics of (DSSCs) based on electrolytes containing different content (0 wt%, 1 wt%, 2 wt%, 4 wt%, 6 wt%, 8 wt%) of TiO₂ which were measured under AM 1.5 solar spectrum irradiation of 100 mW.cm⁻² are shown in Fig. 3.

The data of the open circuit voltage (V_{oc}), short circuit current density (J_{sc}), fill factor (FF) and the photoelectric conversion efficiency (η) are also summarized and listed in Table 2. Electrolyte in (DSSCs) without TiO₂ shows a (J_{sc}) of 5.86 mA cm⁻², (V_{oc}) of 0.68 mV, (FF) of 0.76, and (η) of 1.24% respectively. The maximum values of (J_{sc}), (V_{oc}) and (η) are obtained by increasing the content of TiO₂ to 4 wt%, but these values decrease with additional TiO₂. The best performance of (DSSCs) was obtained from electrolyte which containing 4 wt% TiO₂ which shows a maximum photoelectric conversion efficiency of 7.46%. The performance of the (DSSCs) devices decrease with the excess addition of TiO₂ into the (IL) based gel electrolyte, probably due to the high viscosity of the gel electrolyte and the

aggregation of TiO₂ which blocked the charge transfer in the gel electrolyte.

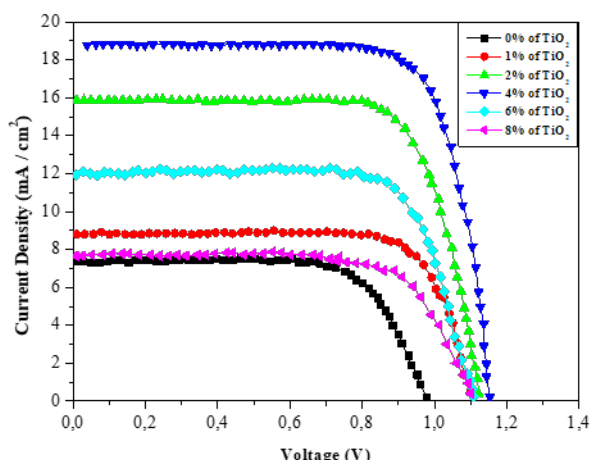


Figure 3. J-V curves of DSSCs with electrolytes content (0 wt%, 1 wt%, 2 wt%, 4 wt%, 6 wt%, 8 wt%) of TiO₂ under simulated AM 1.5 solar spectrum irradiation at 100 mW cm⁻²

The higher charge density in the (DSSCs) might be due to the higher thermal stability of poly (IL), which will be beneficial for durable high temperature (DSSCs). It should be noted that the efficiency of the (DSSCs) is critically dependent on the ion conductivity and diffusion coefficient of the anions in (IL), which the π - π stacked imidazolium rings of the Poly(IL) provide the charge transport from the counter electrode to the photoanode [40, 41].

3.5. Incident photo-to-current conversion efficiency

Figure 4 shows the incident photo-to-current conversion efficiency (IPCE) curves of cells content (0 wt%, 1 wt%, 2 wt%, 4 wt%, 6 wt%, 8 wt%) of TiO₂. Cell content (4 wt%) have high (IPCE) value as 78.8% at 550 nm was obtained, which is higher than that of Cell content (0 wt%) which have (16.8%), Cell (1 wt%) (36.2%), Cell (2 wt%) (54.6%), Cell (6 wt%) (38.3%), and Cell (8 wt%) (19.7%) respectively. The photoelectric conversion efficiency of the (DSSCs) is consistent with the (IPCE) values.

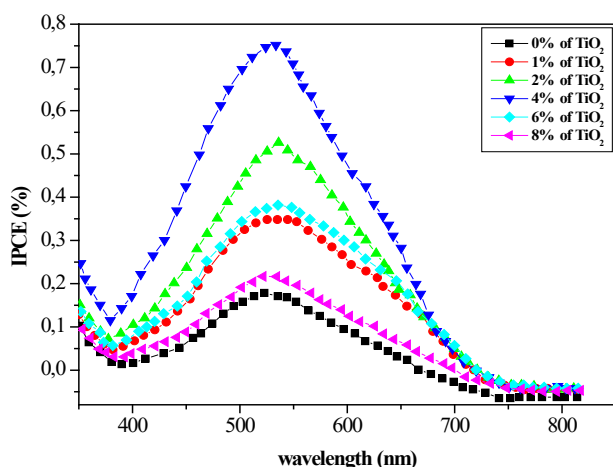


Figure 4. IPCE curves of DSSCs based on gel electrolytes content (0 wt%, 1 wt%, 2 wt%, 4 wt%, 6 wt%, 8 wt%) of TiO₂

These indicate that the weak interaction force between the alkyl chain of the imidazolium cation and its flexibility enables the electron to be easily transferred in the electrolyte [40]. Thus, the ionic conductivity and diffusion coefficient of PF₆⁻ in the poly(IL) based gel electrolyte still reached reasonable values.

3.6. Electrochemical impedance spectroscopy (EIS) measurements

The electronic and ionic processes occurring in (DSSCs) were investigated by the electrochemical impedance spectroscopy (EIS) technique. The (EIS) Nyquist plot of cells content (0 wt%, 1 wt%, 2 wt%, 4 wt%, 6 wt%, 8 wt%) of TiO₂ which measured at -0.7V bias under dark environment were shown in Fig. 5.

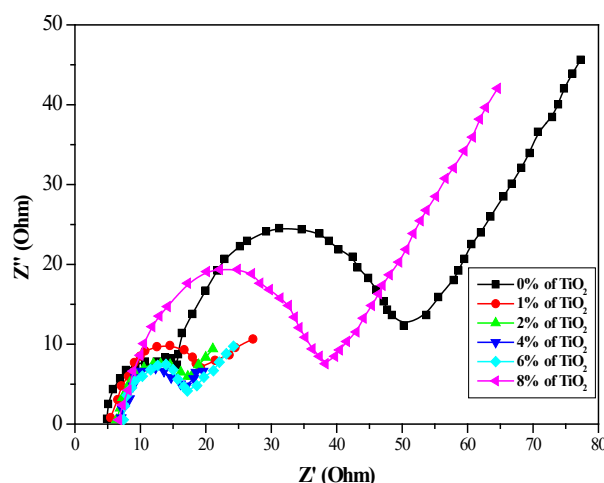


Figure 5. EIS Nyquist plots of cell content (0 wt%, 1 wt%, 2 wt%, 4 wt%, 6 wt%, 8 wt%) of TiO₂.

In the (EIS) spectra of (DSSCs) from high to low frequency three semicircles can be seen correspond to the charge transfer resistance at the counter electrode (R_1), the resistance of IZO coated FTO glass substrate, TiO₂ doped electrolyte interface (R_2), and the Warburg diffusion process (R_{diff}) of PF₅⁻/PF₆⁻ in the electrolyte respectively [42, 43]. The overall series resistance was coded as (R_s). The values corresponding of the resistance shown in Fig.5 are listing in Table 2.

Table 2. Electrochemical impedance spectroscopy results of cells content (0 wt%, 1 wt%, 2 wt%, 4 wt%, 6 wt%, 8 wt%) of TiO₂

Cells content TiO ₂ (wt%)	R ₁ (Ω)	R ₂ (Ω)	R _{diff} (Ω)
0 wt%	12.24	10.24	28.18
1 wt%	7.12	5.86	8.78
2 wt%	5.56	2.31	4.64
4 wt%	3.86	1.89	2.64
6 wt%	6.26	2.94	9.14
8 wt%	7.89	6.16	21.04

The maximum values of (R_1) was obtained by increasing the content of TiO₂ to (8 wt%), but the value decrease with additional TiO₂. This phenomenon is in good coordination

with the reversed order observed for the (η) of the (DSSCs). The trends of (R_2) and (R_{diff}) are similar with (R_1), the minimum resistance values of 1.89 and 2.64 Ω were shown in cell content (4 wt%) of TiO₂. These results conforming that the charge transport at the IZO /electrolyte interface increased, as well as the enhancement of transport of PF₅⁻/PF₆⁻ ions in the electrolyte by the addition of proper content of TiO₂, which reducing the charge recombination at photoanode /electrolyte interface due to the enhanced charge transport properties of an PF₅⁻/PF₆⁻ redox couple in the gel electrolyte.

3.7. Intensity-modulated photocurrent and photovoltage spectroscopy measurements

To further investigate the TiO₂ content effect on the electron transport and charge recombination in the DSSCs, plots of intensity- modulated photocurrent spectroscopy (IMPS) (Figure 6.A) and photovoltage spectroscopy (IMVS) (Figure 6.B) of cells contents (0 wt%, 1wt%, 2 wt%, 4 wt%, 6 wt%, 8 wt%) of TiO₂ were conducted. The transit time (τ_d) and electron lifetime (τ_n) can be calculated using the follow equations:

$$\tau_d = (2\pi f_{min}(IMPS))^{-1} \quad (1)$$

$$\tau_n = (2\pi f_{min}(IMVS))^{-1} \quad (2)$$

Where: $f_{min}(IMPS)$ and $f_{min}(IMVS)$ are the frequencies at the minimum imaginary component in the (IMPS) and (IMVS) plots [38].

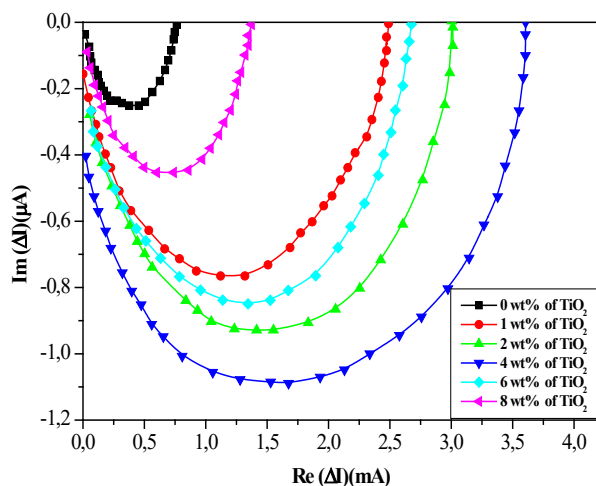


Figure 6. A. IMPS plots of cell content (0 wt%, 1wt%, 2 wt%, 4 wt%, 6 wt%, 8 wt%) of TiO₂

The electron lifetime and transit time of cells contents (0 wt%, 1wt%, 2 wt%, 4 wt%, 6 wt%, 8 wt%) of TiO₂ were listed in Table 3. The longest electron lifetime of 114.89 ms and the shortest transit time of 0.34 ms were showed by cell content (4 wt%) of TiO₂. the collection of electrons were favouring by a long (τ_n) before they recombine in the cells [39], and indicating more electrons surviving from the back reaction which results in high photocurrent [38, 40].

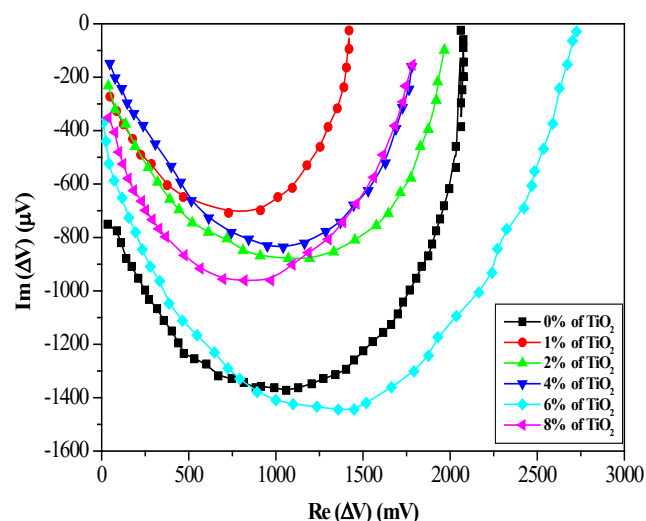


Figure 6.B. IMVS plots of cell content (0 wt%, 1wt%, 2 wt%, 4 wt%, 6 wt%, 8 wt%) of TiO₂

To collect the charge injected by dye in (DSSCs) [41], it is important the (τ_d) is much shorter than (τ_n) which confirming our results. The performance of (DSSCs) is improved by increasing the content of TiO₂ until it reaches 4 wt% which give a tendencies of (τ_n) and (τ_d) in good agreement.

Table 3. IMPS/IMVS parameters of cells content (0 wt%, 1wt%, 2 wt%, 4 wt%, 6 wt%, 8 wt%) of TiO₂

Cells content TiO ₂ (wt%)	$f_{min}(IMPS)$ (Hz)	$f_{min}(IMVS)$ (Hz)	τ_d (ms)	τ_n (ms)
0 wt%	8.76	18.22	16.55	13.72
1 wt%	26.1	6.24	9.86	38.25
2 wt%	55.37	3.12	5.74	82.61
4 wt%	76.14	0.86	0.34	114.89
6 wt%	38.94	4.48	4.32	50.59
8 wt%	18.22	10.23	12.43	21.06

Compared with Cell content (0 wt%) of TiO₂, composite gel electrolytes of (DSSCs) are enough to favors electron transport through a longer distance with less diffusive hindrance which leads finally to enhanced photoelectric conversion efficiency [42].

3.8. Efficiency for the DSSCs aging tests

For the practical applications of (DSSCs), the long-term stability still as major problem. So we have investigated the long-term stability of (DSSCs) via an accelerating aging test of the sealed devices [49]. The values of the total efficiencies of cell content (0 wt%, 4 wt%, 8 wt%) of TiO₂ measured on the first day are shown in Fig.7. The early stage of long-term stability testing of the efficiency of all the three devices was enhanced by the increased of the dye regeneration rate which enhanced the (J_{sc}) of (DSSCs) [47, 48]. As shown in Fig. 7, after 1600 h Cells content (4 wt%) and (8 wt%) of TiO₂ were retains 98.5% and 94% of their initial efficiency respectively, under the same conditions cell content (0 wt%) of TiO₂ maintained 85% of the initial efficiency.

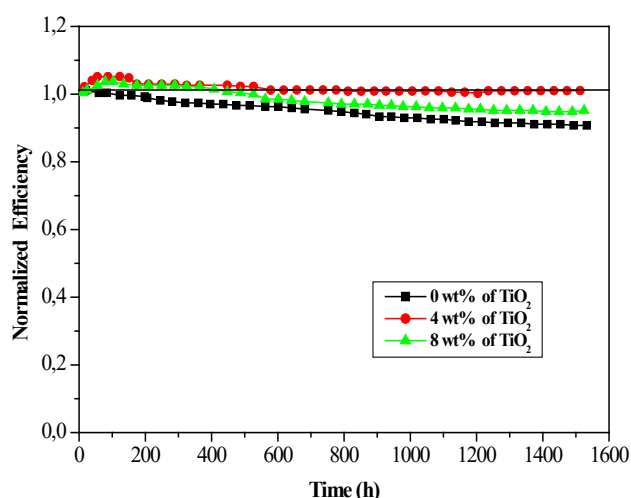


Figure.7. Time-course variation of the normalized efficiency for the DSSCs with cells content (0 wt%, 4 wt%, 8 wt%) of TiO₂ during accelerated aging tests at 60 °C of.

By addition of TiO₂ the long-term stability of (DSSCs) is greatly improved, probably due to the gel network hindered the leakage in the release of ionic liquid component from the composite electrolyte, it should be noted that both the poly (IL) electrolytes exhibit superior long-term stability than the ionic liquid electrolyte because the gel network hindered the leakage of the liquid electrolyte effectively [40]. The long-term stability of cell content (8 wt%) is lower than the cell content (4 wt%) of TiO₂, probably due to the aggregation of TiO₂ in the electrolyte [42]. All these results have excellent practical stability of the (DSSCs) based on this type of gel electrolyte containing proper content of TiO₂.

4. CONCLUSION

Indium doped ZnO (IZO) coated FTO Glass substrates exhibited a particularly high transparency. X-ray diffraction investigations showed that the FTO glass was highly textured, and IZO films coated FTO glass substrate prepared high-quality. Poly (IL)/IL/TiO₂ composite gel electrolyte have been prepared for quasi-solid state (DSSCs) with various amounts of TiO₂. The incorporation of proper amount of TiO₂ in the composite electrolytes increased the conductivities, this explained the enhancement in the charge transport at the TiO₂ /electrolyte interface, as well as the enhancement of transport of PF₅⁻/PF₆⁻ ions. The composite electrolytes in (DSSCs) with proper TiO₂ show higher open circuit voltage (Voc), short circuit current density (Jsc), photoelectric conversion efficiency (η), and better long-term stability compared with the (DSSCs) based on electrolyte without TiO₂. The maximum efficiency of the (DSSCs) based on composite electrolyte showed high value 7.46% in 4 wt% of TiO₂ under AM 1.5 solar spectrum irradiation. All the obtains results in the present work have excellent practical stability of the (DSSCs) based on this type of gel electrolyte containing proper content of TiO₂ which could overcome the leakage problem of liquid electrolytes.

REFERENCES

- [1] M.S. Su'ait, M.Y.A. Rahman, A. Ahmad, (2015). Review on polymer electrolyte in dye-sensitized solar cells (DSSCs). *Sol. Energy*, 115, 452–470.
- [2] M. Laura Parisi, S. Maranghi, A. Sinicropi, R. Basosi, Development of Dye Sensitized Solar Cells: A Life Cycle Perspective for The Environmental and Market Potential Assessment of a Renewable Energy Technology, *Journal of New Materials for Electrochemical Systems*, 7(2013)143-148, DOI: <https://doi.org/10.18280/ijht.310219>.
- [3] K. Mohan, A. Bora, B.C. Nath, P. Gogoi, B.J. Saikia, S.K. Dolui, (2016). A highly stable and efficient quasi solidstate dye sensitized solar cell based on Polymethylmethacrylate (PMMA)/Polyaniline Nanotube (PANI-NT) gel electrolyte. *Electrochim. Acta*, 222, 1072–1078.
- [4] S.S. Yuan, Q.W. Tang, B.L. He, P.Z. Yang, (2014). Efficient quasi-solid-state dye-sensitized solar cells employing polyaniline and polypyrrole incorporated microporous conducting gel electrolytes. *J. Power Sources*, 254, 98–105.
- [5] R.H. Lee, T.F. Cheng, J.W. Chang, Ho, J.H.(2011). Enhanced photovoltaic performance of quasi-solid-state dye-sensitized solar cells via incorporating quaternized ammonium iodide-containing conjugated polymer into PEO gel electrolytes. *Colloid Polym. Sci.*, 289, 817–829.
- [6] L. Shuang, L. Liu, M. Qingzhuo Du Zeyuan, F. Yuhang, Z. Yajun, L. Xiaowei, Z. Xiaohui, Preparation of PbS/NiO Composite Photocathode and Their Applications in Quantum Dot Sensitized Solar Cells, *Journal of New Materials for Electrochemical Systems*, 23(2020)7-12. DOI: <https://doi.org/10.14447/jnmes.v23i1.a02>.
- [7] H.A. Deepa, G.M. Madhu, B.E. Kumara Swamy, J. Koteswararao, Estimation of Photovoltaic Properties of ZnO nanoparticles and CeO₂- ZnO composite and Electrochemical Determination of Adrenaline Employing Voltammetry Studies, *Journal of New Materials for Electrochemical Systems*, 23(2020)71-77. DOI: <https://doi.org/10.14447/jnmes.v23i2.a03>.
- [8] Q.H. Li, X.X. Chen, Q.W. Tang, H.Y. Cai, Y.C. Qin, B.L. He, M.J. Li, S.Y. Jin, Z.C. Liu, (2014), Enhanced photovoltaic performances of quasi-solid-state dye sensitized solar cells using a novel conducting gel electrolyte. *J. Power Sources*, 248, 923–930.
- [9] K. Tennakone, G.R.R.A. Kumara, A.R. Kumarasinghe, K.G.U. Wijayantha, P.M. Sirimanne, A dye-sensitized nano-porous solid-state photovoltaic cell. *Semicond. Sci. Technol.* 1995, 10, 689–1693.
- [10] G. Kumara, A. Konno, K. Shiratsuchi, J. Tsukahara and K. Tennakone, *Chem Mater*, 2002, 14, 954–955.
- [11] K. Tennakone, G. Senadeera, D. De Silva and I. Kottegoda, *Appl Phys Lett*, 2000, 77, 2367–2369.
- [12] G.R.R. Kumara, A. Konno, G.K.R. Senadeera, P.V.V. Jayaweera, D.B.R.A. De Silva, K. Tennakone, Dye-sensitized solar cell with the hole collector p-CuSCN deposited from a solution in n-propyl sulphide. *Sol. Energy Mater. Sol. Cells*. 2001, 69, 195–199
- [13] C. S. Karthikeyan, H. Wietasch and M. Thelakkat, *Adv Mater*, 2007, 19, 1091–1095.

- [14] U. Bach, D. Lupo, P. Comte, J. Moser, F. Weissörtel, J. Salbeck, H. Spreitzer and M. Grätzel, *Nature*, 1998, 395, 583- 585.
- [15] A. Sepehrifard, B. A. Kamino, T. P. Bender and S. Morin, *ACS Appl Mater Interfaces*, 2012, 4, 6211–6215
- [16] M. Wang, X. Pan, X. Fang, L. Guo, C. Zhang, Y. Huang, Z. Huo and S. Dai, *J Power Sources*, 2011, 196, 5784–5791.
- [17] B. O'Regan, D.T. Schwartz, Large enhancement in photocurrent efficiency caused by UV illumination of the dye-sensitized heterojunction TiO₂/RuLL NCS/CuSCN: Initiation and potential mechanisms. *Chem. Mater.* 1998, 10, 1501–1509.
- [18] S.E. Shaheen, C.J. Brabec, N.S. Sariciftci, F. Padinger, T. Fromherz, J.C. Hummelen, (2001). 2.5% efficient organic plastic solar cells. *Appl. Phys. Lett.* 78, 841.
- [19] N.F. Zain, N.A. Dzulkurnain, A. Ahmad, F. Salleh, N.S. Mohamed, *Polymer Electrolytes Based on Novel Poly(Ethyl Methacrylate-co-Deproteinized Natural Rubber) for dye Sensitized Solar Cell Application*, *Journal of New Materials for Electrochemical Systems*, 22 (2019) 65-69. DOI: <https://doi.org/10.14447/jnmes.v22i2.a01>
- [20] J.X. Zhao, S.G. Jo, D.W. Kim, (2014), Photovoltaic performance of dye-sensitized solar cells assembled with electrospun polyacrylonitrile/silica-based fibrous composite membranes. *Electrochim. Acta*, 142, 261–267.
- [21] S.H. Park, D.H. Won, H.J. Choi, W.P. Hwang, S.I. Jang, J.H. Kim, S.H. Jeong, J.U. Kim, J.K. Lee, M.R. Kim, (2011), Dye-sensitized solar cells based on electrospun polymer blends as electrolytes. *Sol. Energy Mater. Sol. Cells*, 95, 296–300.
- [22] A. Benabdellah, H. Belarbi, H. Ilikti. (2018). Doping of PANI by ionic liquids and its applications in the junctions. *Book*.
- [23] A. Benabdellah, H. Belarbi, H. Ilikti, T. Benabdallah and M. Hatti. (2015). Magnetic Properties of Polyaniline/ZFe₂O₄ Nanocomposites Synthesized in CTAB as Surfactant and Ionic Liquid. *Tenside Surfactants Detergents*, Vol 52, 431-431.
- [24] G. Wang, L. Wang, S. Zhuo, S. Fang and Y. Lin, *Chem Commun*(2011), 47, 2700–2702.
- [25] Y. Zhou, W. Xiang, S. Chen, S. Fang, X. Zhou, J. Zhang and Y. Lin, *Chem Commun*, (2009), 3895-3897.
- [26] Y. Zhang, J. Zhao, B. Sun, X. Chen, Q. Li, L. Qiu and F. Yan, *Electrochim Acta*, 2012, 61, 185-190.
- [27] A. Benabdellah, M. Debdab, Y. Chaker, B. Fetouhi, M. Hatti. (2019). Efficiency of Polyaniline/(ZnO, Cd) Junctions Doped by Ionic Liquid in Photovoltaic Properties. *International Conference on Artificial Intelligence in Renewable Energetic Systems. IC-AIRES2019*.
- [28] G. Wang, L. Wang, S. Zhuo, S. Fang and Y. Lin, *Chem Commun* 2011, 47, 2700–2702.
- [29] Y. Zhang, J. Zhao, B. Sun, X. Chen, Q. Li, L. Qiu and F. Yan, *Electrochim Acta*, 2012, 61, 185-190.
- [30] Y. Zhou, W. Xiang, S. Chen, S. Fang, X. Zhou, J. Zhang and Y. Lin, *Chem Commun*, 2009, 3895-3897.
- [31] A. Mahdjoub, S. Benzitouni and M. Zaabat. (2018). High transparency of ZnO: In coated glass substrates. *Journal of New Technology and Materials (JNTM)*. Vol. 08, N°01, 31-36
- [32] B. Fetouhi, H. Belarbi, A. Benabdellah, S. Kasmi-Mir, G. Kirsch. (2016), Extraction of the heavy metals from the aqueous phase in ionic liquid 1-butyl-3-methylimidazolium hexafluoro-phosphate by N-salicylideneaniline. *J. Mater. Environ. Sci.* 7 (3) 746-754.
- [33] Y. Chaker, The influence of chloride and hydrogen sulfate anions in two polymerised ionic liquids based on the poly(1-(hydroxyethyl)-3-vinylimidazolium cation, synthesis, thermal and vibrational studies. *European Polymer Journal*. Vol 108, (2018) 138-149
- [34] BC. Jiao, XD. Zhang, CC. Wei (2011), Effect of acetic acid on ZnO: in transparent conductive oxide prepared by ultrasonic spray pyrolysis. *Thin Solid Films* 520:1323–1329. doi:10.1016/j.tsf.2011.04.152
- [35] H. Gómez, A. Maldonado, R. Asomoza, (1997), Characterization of indium-doped zinc oxide films deposited by pyrolytic spray with different indium compounds as dopants. *Thin Solid Films* 293:117–123. doi:10.1016/S0040-6090(96)09001-3
- [36] J. Wienke, AS. Booij, (2008), ZnO: in deposition by spray pyrolysis — Influence of the growth conditions on the electrical and optical properties. *Thin Solid Films* 516:4508–4512. doi:10.1016/j.tsf.2007.05.078
- [37] S. Hyung Kang, K. Jae-Yup, K. Yukyeong, K. Hyun Sik, S. Yung-Eun, Surface Modification of Stretched TiO₂ Nanotubes for Solid-State Dye-Sensitized Solar Cells. *J. Phys. Chem. C* 2007, 111, 26, 9614-9623
- [38] J. Bisquert. Comment on Diffusion Impedance and Space Charge Capacitance in the Nanoporous Dye-Sensitized Electrochemical Solar Cell and Electronic Transport in Dye-Sensitized Nanoporous TiO₂ Solar Cells- Comparison of Electrolyte and Solid-State Devices. *J. Phys. Chem. B* 2003, 107, 48, 13541-13543.
- [39] H.J. Lee, K. JinLee, K. Mi-Ra, W. S. Shin, S. HoJin, K. Hoon Kim, D. Won Park & S. Wook Park, (2011), Influence of Ionic Liquids in Quasi-Solid State Electrolyte on Dye-Sensitized Solar Cell Performance. *Journal Molecular Crystals and Liquid Crystals*. Volume 462, 75-81.
- [40] K. Jeong-Hwa, J. Kun-Ho, S. Shi-Joon, H. Dae-Kue. (2017), Enhanced Performance of Dye-Sensitized Solar Cells Based on Electrospun TiO₂ Electrode. *Journal of Nanoscience and Nanotechnology*, Vol 17, 8117-8121.
- [41] O. Borodina and T. R. Jow, Quantum Chemistry Studies of the Oxidative Stability of Carbonate, Sulfone and Sulfonate-Based Electrolytes Doped with BF₄⁻, PF₆⁻ Anions. *J. Electrochemical Society*. 2011 vol 33 (2011) 77-84.
- [42] B. Lin, H. Shang, F. Chu, Y. Ren, N. Yuan, B. Jia, S. Zhang, Y. Wei, X. Yu and J. Ding, *Electrochimica Acta*, 2014, 134, 209– 214.
- [43] Y. Wang, J. Zhang, X. Cui, P. Yang and J. Zeng, *Electrochim Acta*, 2013, 112, 247-251.
- [44] S. Sharma, O. K. Varghese, G. K. Mor, T. J. LaTempa, N. K. Allam and C. A. Grimes, *J Mater Chem*, 2009, 19, 3895-3898.
- [45] F. Fabregat-Santiago, J. Bisquert, G. Garcia-Belmonte, G. Boschloo and A. Hagfeldt. (2005). *Solar Energy Materials and Solar Cells*, 87, 117-131.

- [46] W. Zhang, C. Yuan, J. Guo, L. Qiu, F. Yan. (2014). ACS Appl Mater Interfaces, 6, 8723–8728.
- [47] X. Chen, J. Zhao, J. Zhang, L. Qiu, D. Xu, H. Zhang, X. Han, B. Sun, G. Fu, Y. Zhang and F. Yan, J Mater Chem, 2012, 22, 18018–18024.
- [48] P. Wang, S. M. Zakeeruddin, J. E. Moser, M. K. Nazeeruddin, T. Sekiguchi and M. Grätzel, Nat Mater, 2003, 2, 402–407.

NOMENCLATURE

[BMIM] PF6	1-butyl-3-methyl-imidazolium hexafluorophosphate
DSSCs	dye-sensitized solar cells
EIS	Electrochemical impedance spectroscopy
FTO	Fluorine Tin Oxide
FIB	focused ion beam
FEG-SEM	Field Emission-Gun-Scanning Electron Microscopy
J _{sc}	short circuit current density
IMPS	intensity- modulated photocurrent spectroscopy
IMVS	Intensity- modulated photovoltage spectroscopy
IPCE	Incident photo-to-current conversion efficiency
IZO	Indium Zinc Oxide
PCl ₅	Phosphorus pentachloride
R ₁	Resistance at the counter electrode
R ₂	Resistance of electrolyte interface
R _{diff}	Resistance diffusion process
TiO ₂	Titanium dioxide
V _{oc}	Open circuit voltage
τ _d	The transit time
τ _n	Electron lifetime
η	Conversion efficiency